ELSEVIER

Thermochimica Acta 264 (1995) 193–203

thermochimica acta

Thermogravimetric studies on temperature programmed desorption of probe molecules from dealuminated clinoptilolite

F. Grejták *, J. Krajčovič, P. Komadel

Institute of Inorganic Chemistry, Slovak Academy of Sciences, 842 36 Bratislava, Slovakia

Received 17 August 1994; accepted 13 March 1995

Abstract

Clinoptilolite was dealuminated by $(NH_4)_2SiF_6$ solution. Three, four and five acid site types were determined by TPD of ammonia, pyridine and n-butylamine, respectively. Dealumination increased the relative amount of weak acid sites. Extraframework aluminium remained in the reaction product and lowered the accessibility of the strong acid sites.

Keywords: Acid sites; Clinoptilolite; Dealumination; Temperature programmed desorption (TPD)

1. Introduction

Temperature programmed desorption (TPD) of probe molecules is frequently used for characterisation of acidic properties of zeolites. The desorption peak in the 653–673 K region of zeolite Beta was found to correlate with the Al content, acidity and catalytic activity [1]. Three peaks were found in TPD spectra of ammonia desorption from NH_4-Y zeolite, while Si-enrichment led to only two poorly resolved peaks [2]. The high-temperature peak (at 475°C) in the TPD spectrum of NH_4-mordenite depended on the structural aluminum content in the mineral [3]. Three different acid sites were found on all NH_3 desorption curves of three zeolites, but the peak temperatures and heat of ammonia desorption varied [4]. Steric factors eclipsed variations in the number or strength of acid sites determined by TPD desorption of

* Corresponding author.

SSDI 0040-6031(95)02343-7

pyridine and ammonia from synthetic mordenites [5]. Thermogravimetric and thermal desorption mass spectroscopic data of amine desorption from various forms of Y-zeolite proved that amines decompose on the zeolitic surface to give rise to various reactions typical for those on acid catalysts.

The number of surface acid sites could be estimated from the number of amine molecules decomposed during thermal desorption [6].

The aim of the present paper was to compare the degree of dealumination and acidic properties of dealuminated clinoptilolite samples, using the TPD technique of probe molecules with different kinetic diameter and basicity.

2. Experimental

2.1. Materials

Rhyolite tuff containing 70 mass% of clinoptilolite (Nižný Hrabovec, Slovakia) was used as starting material. Investigated tuff contains, besides clinoptilolite, about 8 mass% of the feldspars labradorite and/or andesite, 6 mass% of cristobalite and 8 mass% of quartz, and about 8 mass% of amorphous volcanic glass and/or SiO_2. This amount of admixtures, determined by XRD, does not change after the dealumination process, consequently this material (sample D) can be used for studies of relative changes in the number of acid sites of clinoptilolite. The admixtures adsorb only physically gaseous bases, so their influence on the high temperature peaks, which describe acid sites, can be neglected.

The sample was treated with 3 mol dm^{-3} NH_4Cl solution at room temperature three times for 24 h to prepare the NH_4-form. The product was washed with boiling water until negative reaction of silver nitrate solution with chlorides was achieved, then dried at 40 °C (sample D_0). Dealumination was carried out by stirring of NH_4-clinoptilolite in 0.75 mol dm^{-3} $(NH_4)_2SiF_6$ solution at 95 °C for 1, 3, 6, 16 and 24 h (samples D_1-D_{24}). Dealumination was effective yielding Si/FAl (FAl is framework aluminium) ratios of 4.56 to 12.79 for D_0-D_{24} (Table 1). Details for unit cell formulas and framework/extraframework aluminium ratio calculations for dealuminated samples were published elsewhere [7].

Table 1
Si/framework-Al ratio of the dealuminated samples

Sample[a]	D_0	D_1	D_3	D_6	D_9	D_{16}	D_{24}
Si/FAl	4.56	5.05	5.72	6.63	7.11	9.03	12.79

[a] The numbers given in the subscripts show the time of dealumination in hours.

2.2. Adsorption of probe molecules

Liquid NH_3 was saturated with dried KSCN, pyridine (py) and n-butylamine (bu) were used as obtained. All three sorbents were dried over NaA zeolite to remove water. Samples were loaded with probe molecules without previous acid washing. Samples were deammoniated and dehydrated at 450 °C in dynamic vacuum (5 Pa) for 5 h. The probe molecules were adsorbed after cooling 22 ± 2 °C for 24 h at the saturated vapour pressure. Then the samples were outgased at 200 °C for 1 h to remove physically sorbed probe molecules and studied by thermal analysis.

2.3. Acid washing

Dealuminated samples were washed with 4 mol dm^{-3} HCl at room temperature for 1 h to remove extraframework aluminium (EFAl).

2.4. Methods

A Derivatograph Q-1500 (MOM Budapest) was used for DTA, DTG and TG measurements. 560 mg of samples was analysed in air or in N_2 (flow 80 ml min^{-1}) at a heating rate of 20 K min^{-1}. Only a slight shift of DTG and DTA peaks to higher temperatures was observed in N_2 compared to air (Fig. 1).

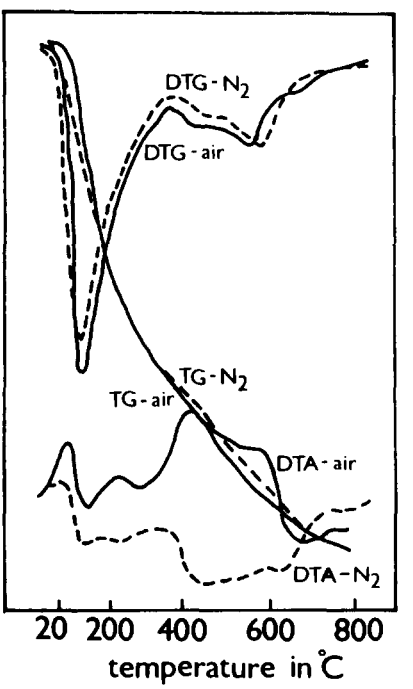

Fig. 1. Comparison of thermoanalytical curves of D_0 sample obtained in air and in N_2.

DTG curves were deconvoluted using Pitha and Jones PC program for decomposition of bands, which optimises temperatures, intensities and half-widths of the component bands [8]. The relative error of the peak area determination in the deconvolution was less than 8% (deconvolution of five various DTG curves from the same sample).

A Netzsch STA-QMS, system 409 thermal analyser was used for qualitative gaseous products analysis. Heating rate 10 K min^{-1} and flow rate of Ar 80 ml min^{-1} were used. The peak positions of the same gaseous products were found within $\pm$ 7 K range.

3. Results and discussion

The best fits for the DTG curves of basis desorption from clinoptilolite samples were obtained with six, five and seven desorption peaks for H_2O and NH_3, bu, and py desorption, respectively (Figs. 2–4). Desorption peaks A in Fig. 2–4 occur approximately at the same temperature for each sample, independently on the base used. Mass spectroscopy analysis of gaseous desorption products (Fig. 5–7) indicate that desorption peaks A in Fig. 2–4 demonstrate the desorption of physically bonded water. However, both NH_3 (m = 17) and H_2O (m = 18) were found in the desorption gases for NH_3 desorption (Fig. 5). Overlapping m = 17 and m = 18 curves occurred also below the evacuation temperature (200°C). The small NH_3 molecules could possibly migrate into the zeolite porous structure. Water in desorption gases is supposed to be due to moisture desorbed from very weak and unoccupied acid sites and can be also associated with exchangeable cations and/or EFAl species. Adsorbed water is supposed to hydrate NH_3 molecules thus supporting their migration in zeolite structure. The temperatures of desorption maxima A are shifted to higher values with increasing dealumination, e.g. from 155°C (D_0) to 182°C (D_{24}) for py and bu, and from 160°C (D_0) to 208°C (D_{24}) for NH_3.

The desorption peaks B were found at about 200°C for NH_3 (Fig. 2), py (Fig. 3), and bu (Fig. 4), respectively. The position change of B-peaks with dealumination was

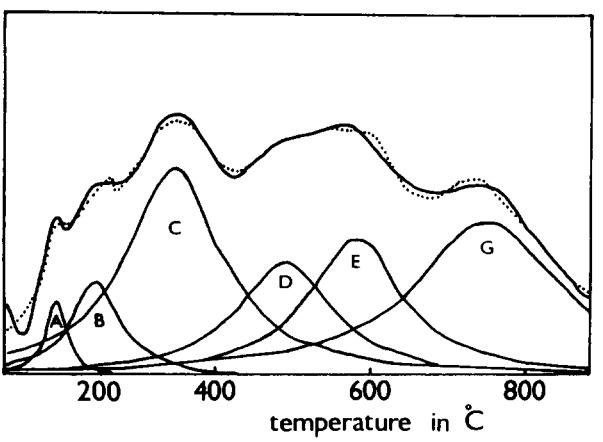

Fig. 2. DTG curve of desorption for NH_3-sorbed D_0 sample and fitted desorption peaks.

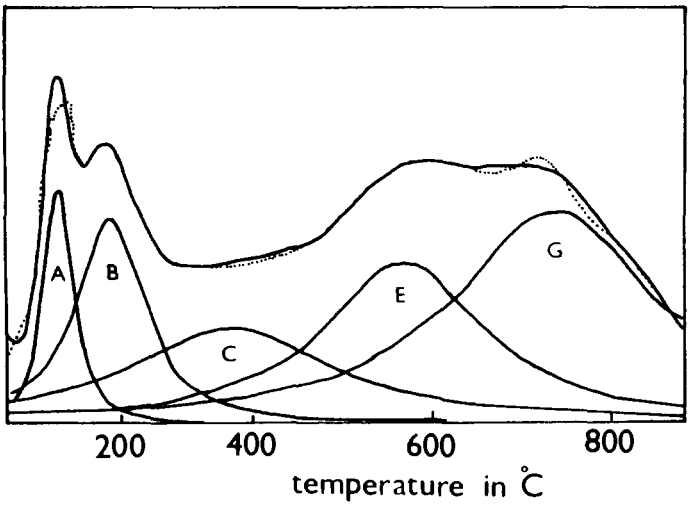

Fig. 3. DTG curve of desorption for pyridine-sorbed D_0 sample and fitted desorption peaks.

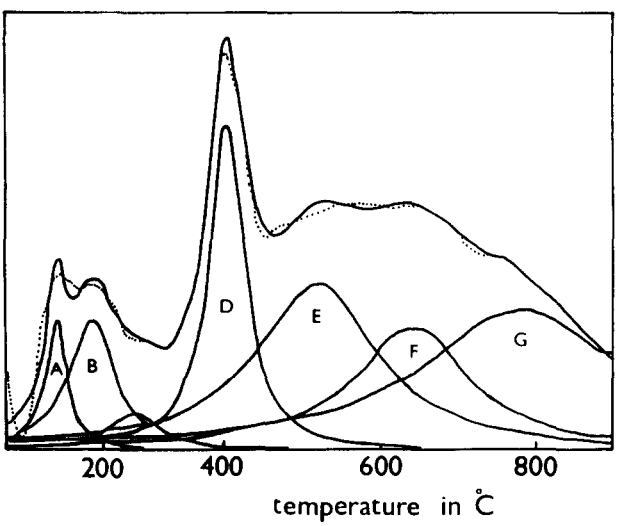

Fig. 4. DTG curve of desorption for n-butylamine-sorbed D_0 sample and fitted desorption peaks.

minor. The mass spectra of desorption products of all three basis (Figs. 5–7) indicate that the B-peaks in Figs. 2–4 are due to combined desorption of water and the bases. The dependence of the desorption peak areas, obtained from the fitting procedure, on the aluminium content in the dealuminated samples is shown in Fig. 8. Assuming that the peak area corresponds to the number of acid sites, the shape of the curve B (Fig. 8)

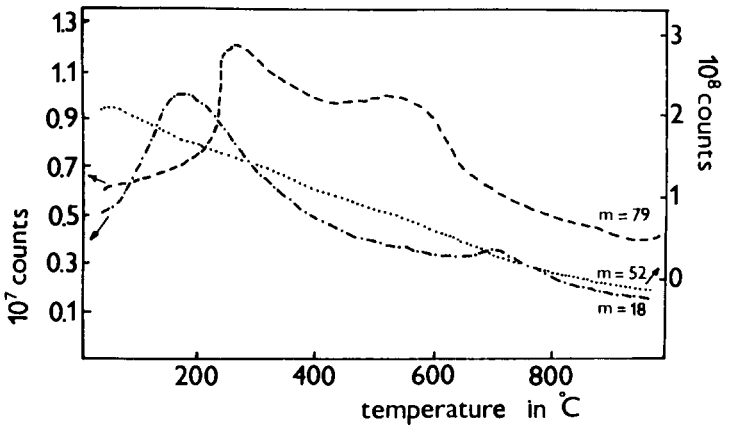

Fig. 5. Mass spectrum of desorption for NH_3-sorbed D_0 sample.

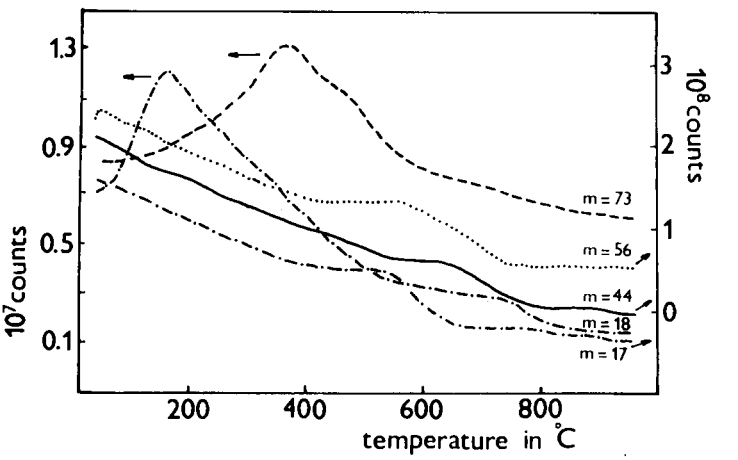

Fig. 6. Mass spectrum of desorption for pyridine-sorbed D_0 sample.

shows increasing amount of acid sites B from D_0 to D_3, then a decrease with dealumination. Lower amount of B–NH_3 acid sites was found after the acid washing of the dealuminated samples (Fig. 8, curves B′ and B). EFAl, retaining in the dealuminated samples after washing with water, was removed by the acid treatment. Molecules of ammonia can be bonded on EFAl in the pores due to the small kinetic diameter (0.26 mm) of NH_3. Therefore they can be bonded to the porous system, partially occupied by EFAl easier than the bigger molecules of py or bu. The maxima on the B-py and B-bu curves (Figs. 9, 10) of D_0 coincide with the highest specific mesopore surface of slightly dealuminated samples [9].

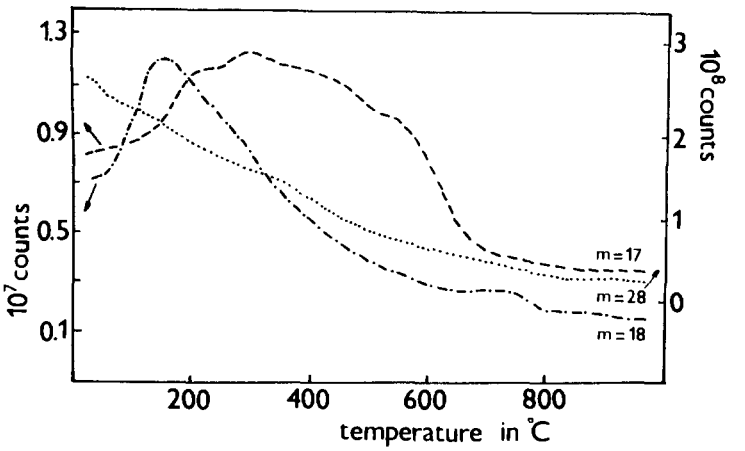

Fig. 7. Mass spectrum of desorption for n-butylamine-sorbed D_0 sample.

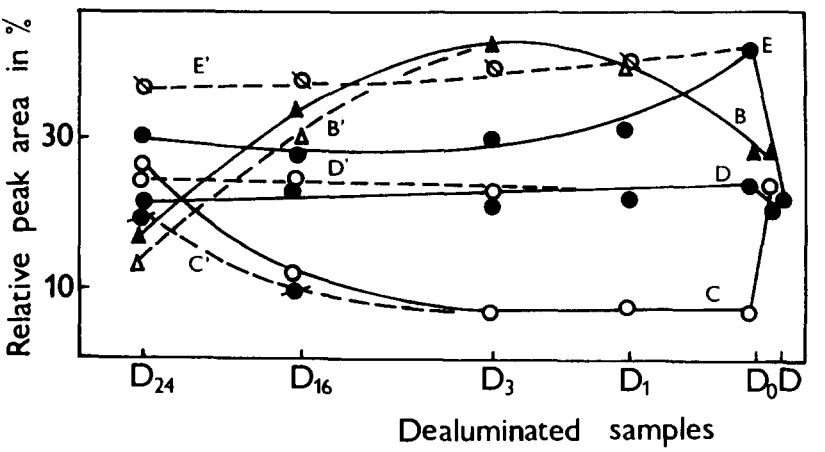

Fig. 8. Relative areas of fitted desorption peaks on DTG curves (see Fig. 2 for D_0) for NH_3-sorbed dealuminated samples.

The peak C positions of NH_3 (Fig. 2) were shifted with dealumination from 370 (D_0) to 350 °C (D_{24}), py (Fig. 3) from 409 (D_0) to 381 °C (D_{24}) and bu (Fig. 4) from 278 (D_0) to 242 °C (D_{24}). The decrease of these temperatures is connected with partial destruction of the pore system, and mesopore formation. The relative mesopore volume increases with dealumination [9], so the diffusion of probe molecules is easier. Low temperature peak C corresponds to desorption of probe molecules from weak acid sites [10–12] according to the scheme:

$$[\text{–OH}...\text{NH}_3] \rightarrow \text{–OH} + \text{NH}_3.$$

The relative number of acid sites C (Figs. 8–10), as determined from the peak areas of desorption of various probe molecules, increased with dealumination in all used

probes. Faster diminution of weak than strong acid sites was reported for deamoniation of dealuminated samples at various temperatures [13]. The changes in the number of acid sites determined after acid washing show the C′ curves in Figs. 8–10. From the C and C′ curves for NH_3, py and bu desorption is assumed that a part of EFAl remaining in the clinoptilolite structure after dealumination, was removed by acid washing. The assignment of peak C was supported by infrared spectroscopic study of dealuminated samples. The intensity of the band at about 3700 cm^{-1}, assigned to stretching vibrations of OH groups associated with EFAl, increased with dealumination [14].

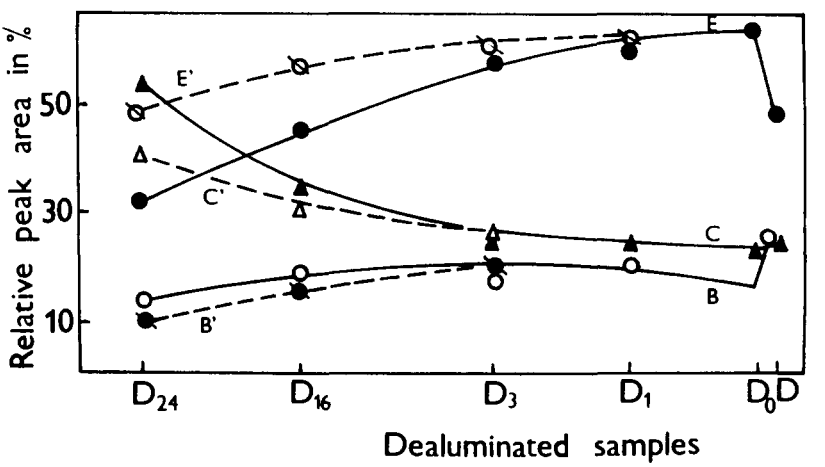

Fig. 9. Relative areas of fitted desorption peaks on DTG curves (see Fig. 3 for D_0) for pyridine-sorbed dealuminated samples.

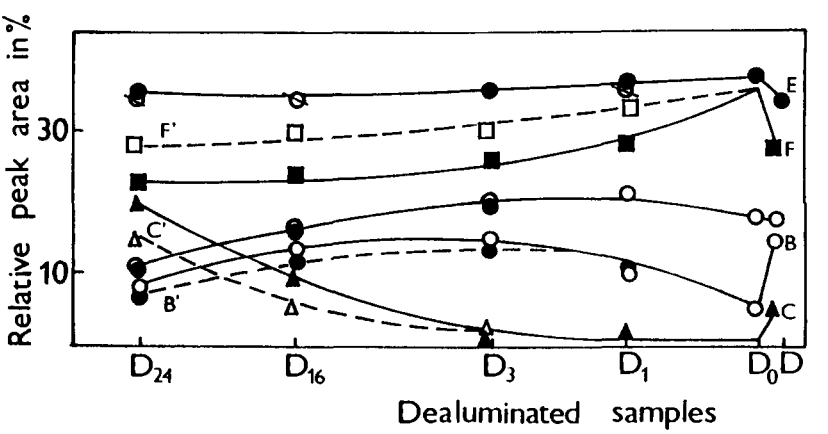

Fig. 10. Relative areas of fitted desorption peaks on DTG curves (see Fig. 4 for D_0) for n-butylamine-sorbed dealuminated samples.

High temperature peaks D, E and F correspond to decomposition of ammonium ions bonded to the strong acid sites [10–12, 14] of clinoptilolite, such as follows:

$$[-O^{\delta-}....NH_4^{\delta+}] \longrightarrow -OH + NH_3,$$

and/or

$$[-OH...O_a^{\delta-}....NH_4^{\delta+}] \longrightarrow -OH + -O_aH + NH_3.$$

The desorption peaks D were fitted for NH_3 and bu desorption (Figs. 2, 4). In the py desorption peak D displays either low intensity or is merged with neighbouring C peaks. Peak D temperatures of NH_3 and bu are at 480°C and 420°C (D_0), respectively (Figs. 2, 4). A shift of these peaks with dealumination to lower temperatures, 450°C and 400°C for D_{24}, respectively, was observed. Mainly NH_3 was detected in desorption gaseous products of NH_3 desorption at these temperatures (Fig. 5). Small amounts of NH_3 (m = 17), butene (m = 56) along with bu (m = 73) were found in the temperature range of D peak in bu desorption (Fig. 7). Presence of NH_3 and butene in bu desorption products is due to Hofmann degradation of butylammonium ions in H-clinoptilolite structure according to scheme:

$$CH_3-(CH_2)_3-NH_3^+\,O^-\text{-zeolite} \longrightarrow NH_3 + CH_3-CH_2-CH=CH_2 + \text{HO-zeolite}$$

Relative D peak areas of NH_3 and bu (Figs. 8, 10) slightly decreased with dealumination. The number of acid sites exhibited no changes after acid treatment for the desorption of n-butylamine, however, a slight increase in the relative D peak area of NH_3 after acid washing of dealuminated samples was observed (Fig. 8).

Desorption peaks E occurred in the deconvolution of the desorption DTG curves for all probe molecules. Their positions were shifted to lower temperatures with increasing dealumination, i.e. from 593 (D_0) to 569°C(D_{24}) for NH_3 (Fig. 2), from 598 (D_0) to 570°C (D_{24}) for py (Fig. 3) and from 550 (D_0) to 528°C (D_{24}) for bu (Fig. 4) Mass spectrum in the E-peak temperature interval of bu (Fig. 7) revealed decreasing n-butylamine content and increasing amount of ammonia and butene in the gaseous desorption products. A small amount of CO_2 and/or propane (m = 44) appeared at about 560°C (Fig. 7) as alternative products of butene cracking reactions. A possible adsorption of Hofmann degradation products on acid sites of formed H-clinoptilolite and the butoxy-groups formation [10] was not confirmed by IR spectroscopy. Only ammonia and pyridine were detected in the temperature region of E-NH_3 and E-py peaks, respectively (Figs. 2, 3, 5, 7). Relative area of desorption peaks E, corresponding to the relative number of strong acid sites, decreased with dealumination for all probe molecules. A significant increase of desorbed NH_3 and py amount was detected after the acid treatment of dealuminated samples (E'-NH_3, E'-py), while the E peak areas of bu exhibited no change after washing with HCl. The effect of acid treatment of dealuminated clinoptilolite on NH_3 and py sorption/desorption is supposed to be due to easier access of strong acid centres for sorption of NH_3 and py after the removal of EFAl by the acid.

Desorption peak F at 635°C (Fig. 4) was fitted only for butylamine desorption. The peak position exhibited no change with dealumination. The presence of n-butylamine,

butene, ammonia, propane and/or CO_2 and water in desorption gases is shown in Fig. 7. The presence of water molecules is due to starting dehydroxylation reaction. The F peak areas decrease with dealumination (Fig. 10). Accessibility of strong acid sites for bu increased after acid treatment of dealuminated samples, as shown by distinction of F-bu and F′-bu curves (Fig. 10).

The presence of three or four different desorption peaks is in agreement with the structural analysis results of clinoptilolite crystals [15]. Four different T–O distances were found for five possible positions of the central tetrahedral cation T(T_1–O and T_2–O distances are the same). The presence of three peaks in NH_3–TPD indicates that two of them (T_4 and T_5) can give rise to acid sites of similar acid strength due to the very similar T–O distances [15].

Desorption peaks G–NH_3, G-py, G-bu (Figs. 2–4) are connected with weight loss due to dehydroxylation of Brønsted acid sites and formation of Lewis sites. Water was found at about 730°C in the desorption gaseous products (Figs. 5–7).

NH_3 is the most convenient probe for the determination of clinoptilolite acid sites due to its small kinetic diameter (0.26 nm) and desorption without decomposition. The number of acid sites, as determined using n-butylamine desorption, is relevant, if the re-adsorption of Hofmann degradation products on zeolite is negligible. Information obtained from pyridine TPD for the determination of clinoptilolite strong acid sites is questionable because of low pK_b and possible intraparticle diffusion effects of py.

4. Conclusions

Adsorption of probe molecules and their subsequent desorption provide information on the acid sites of dealuminated zeolites.

Hot 0.75 M ammonium hexafluorosilicate solution removes aluminium from clinoptilolite structure. This reaction is accompanied by mesopore formation and by shifts of temperatures of C, D and E peaks to lower values. A part of the reaction products remains in the pore system of dealuminated samples probably in the form of an aluminium oxo-hydroxo complex. This complex is assigned as EFAl and can be partially removed by acid treatment.

EFAl has the same effect on the sorption of probe molecules as the exchangeable cations in clinoptilolite, i.e.:

- it shifts the A and B-desorption peaks to higher temperatures,
- it is able to adsorb the probe molecules as weak acid sites (B and C-peaks) and,
- it decreases the accessibility of strong acid sites for probe molecule adsorption.

References

[1] S.G. Hegde, R. Kumar, R.N. Bhat and P. Ratnasamy, Zeolites, 9 (1989) 231.
[2] B.M. Lok, B.K. Marcus and C.L. Angel, Zeolites, 6 (1986) 185.
[3] B.L. Meyers, T.H. Fleisch, G.J. Ray, J.T. Miller and J.B. Hall, J. Catal., 110 (1988) 82.
[4] A. Auroux, Y.S. Jin, J.C. Vedrine and L. Bentoist, Appl. Catal., 36 (1988) 323.

[5] M. Kojima, M.W. Rautenbach and C.T. O'Connor, J. Catal., 112 (1988) 495.
[6] R.V. Jasra, D.B. Bhatt, V.N. Garg and S.G.T. Bhat, Thermochim. Acta, 128 (1988) 115.
[7] F. Grejták, J. Krajčovič and P. Komadel, Geologica Carpathica, Ser. Clays, 45 (1994) 99.
[8] J. Pitha and R.N. Jones, Canad. J. Chem., 44 (1966) 3031.
[9] F. Grejták, P. Hložek, J. Kozánková and J. Krajčovič, Geologica Carpathica, Ser. Clays, 43 (1992) 129.
[10] L. Basini, U. Cornaro and A. Aragno, Langmuir, 8 (1992) 2172.
[11] E.H. Teunissen, F.B.V. Duijneveldt and R.A.V. Jansen, J. Phys. Chem., 96 (1992) 366.
[12] E.H. Teunissen, R.A.V. Jansen and A.P.J. Santen, J. Phys. Chem., 97 (1993) 203.
[13] F. Grejták, I. Horváth and M. Kubranová, Thermochim. Acta, 207 (1992) 209.
[14] H. Pfeifer, Colloids Surfaces, 36 (1989) 169.
[15] T. Armbruster and M.E. Gunter, Amer. Mineral., 76 (1991) 1872.